Computer Assisted Methods in Engineering and Science, **20**: 309–323, 2013.

TWENTY YEARS OF THE CAMES

Examination of mechanical properties of graphene allotropes by means of computer simulation

Adam Mrozek
AGH University of Science and Technology
al. Mickiewicza 30, 30-059 Kraków, Poland
e-mail: amrozek@agh.edu.pl

Tadeusz Burczyński
Institute of Fundamental Technological Research, Polish Academy of Sciences
Pawińskiego 5B, 02-106 Warszawa, Poland

The effective mechanical properties and the stress-strain relations of the eight types of the graphene allotropes are presented in this paper. Series of the tensile and shear tests are performed using the non-equilibrium molecular dynamics (NEMD) and the adaptive intermolecular reactive bond order (AIREBO) potential. The methodology of the investigation as well as obtained results are explained and discussed in detail. Where possible, the achieved results are compared with the data available in the scientific literature in order to validate our molecular dynamics models and simulations. In other cases, i.e., where only information about structural or electronic properties is available, presented results can complement the knowledge about these particular planar carbon networks.

Keywords: graphene, nanomechanics, molecular dynamics, mechanical properties.

1. Introduction

Carbon atoms can exist in one of three possible hybridization states. Thus, they are able to form various types of bondings and spatial configurations. Due to this feature, carbon has many allotropes: the ones occurring naturally such as diamond, graphite and amorphous phase, as well as numerous synthetic structures like graphene, nanotubes and their derivatives. The methods of discovery, synthesis and analysis of the new carbon allotropes are willingly undertaken subject of interest in the recent years [7, 8, 10, 19, 21, 24, 29, 34, 37] because of unique electronic, thermal and mechanical properties of these structures [10, 23, 28].

Several approaches of investigation of the properties of carbon allotropes have been developed. The most popular ones are based on the various *ab-initio* computations [10, 17, 37], molecular dynamics (MD) [7, 8], Cauchy-Born rule [1] and the so-called braced-truss models [28] which can be classified as a particular case of the molecular static's problem [5]. In this work, the mechanical characteristic and properties of the eight planar carbon networks – allotropes of the graphene – were investigated and presented. The results were determined using non-equilibrium molecular dynamics (NEMD) method [12, 25, 33] and the AIREBO potential [31]. The methodology of investigation, as well as achieved results were analyzed and discussed in detail. In the case of graphene and *graphyne* structures comparisons with the available data from the open access literature were also performed [7, 8, 17, 23, 28]. For the rest of the examined lattices, only structural and electronic parameters were found [2, 4, 10, 13, 21, 36]. The purpose of this article is to present the methodology and possibilities of investigation of the mechanical properties of the various flat carbon networks using classical molecular dynamics and the reactive bond order potentials parameterized for hydrocarbons. The second goal of the paper is to deliver effective mechanical properties of the graphene allotropes

which complement the structural and electronic information available in the literature and to extend our knowledge about these materials. Additionally, presented features of the novel carbon-based materials can be helpful nano-engineering applications or in the multi-scale modeling and numerical homogenization.

2. Atomistic structures

The basic graphene structure and eight various allotropes were taken into investigation. Atomistic planar lattices of these materials along with unit cells are presented in Fig. 1. In the further description, all these structures will be referenced in the abbreviated way, as types (A)-(I). Graphene lattice (A) consists of the sp^2 hybridized carbon atoms arranged in a honeycomb-like structure of aromatic benzene rings. It is a simple hexagonal lattice with a triclinic unit cell. Another well-known [2, 7, 21] allotrope is the *graphyne* (B). This structure is built of benzene rings connected by single and triple carbon bonds, forming so-called acetylene linkages (-C≡C-) between sp^2 and sp^1 hybridized atoms, respectively. These two allotropes are chosen for the investigation, due to large amount of information available in the scientific literature. The properties of the *graphene* and *graphyne* are determined using many different methods (*ab-initio*, MD, lattice mechanics) [7, 8, 11, 17, 28], thus these structures are good candidates for validating our molecular dynamics routines and models. Other, similar lattices can be constructed on the basis of *graphyne*, e.g., by simple increasing the length of the acetylene linkages (to -C≡C≡C≡C-), the allotrope called *graphidyne* (C) can be obtained [13]. In the same manner the graphene honeycomb-like structure can be extended with acetylenic chains to the form (D), called *supergraphene* [10]. Two other types of the planar carbon

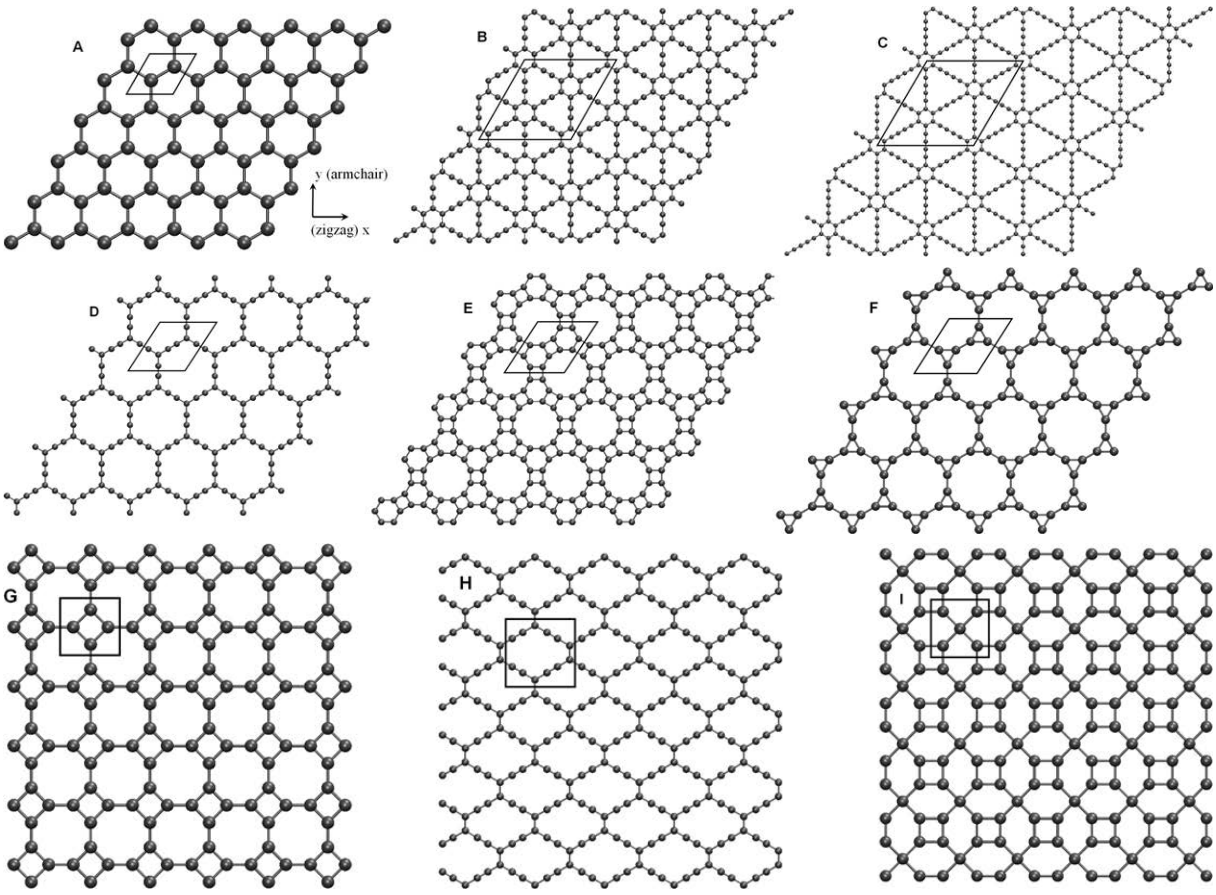

Fig. 1. Atomic structures of the investigated graphene allotropes: A – graphene, B – graphyne, C – graphidyne, D – supergraphene, E, F – structures based on dodecagons, G – octagonal network, H and I – structures made of distorted hexagons. See text for details.

structures (E) and (F) are based on the various arrangements of the dodecagons. The lattice (E) can be decomposed into the system of hexagons and squares, which form the unit cell.

Both of the described above allotropes have similar to graphene, hexagonal lattices and symmetries with triclinic unit cells. The second group which is taken under investigations, are the planar carbon networks built on the basics of the rectangular lattices. The allotrope (G) consists of the sp^2 hybridized carbon atoms arranged in octagons [10, 36] or, from the other point of view, as a lattice made of the square four-atom unit cells. The last two structures (H) and (I) utilize sp^2/sp^1 and sp^2/sp^3 hybridization types, respectively. In both cases, atoms are formed into distorted hexagons. The lattice (H) is similar to the (D), with the vertical acetylenic linkages replaced with the double bounds between sp^2 hybridized carbon atoms. The allotrope (H) has a rectangular unit cell while the variant (I) has a square one.

3. Methodology

Estimation of the mechanical properties of the atomic system at the nonzero temperature can be done by performing MD simulations of the tensile and shearing tests. The classical approach is based on the following four steps.

1. Equilibration of the undeformed investigated molecular model at desired temperature.
2. Application of the finite deformation/load to the atomic system.
3. Equilibration of the deformed/loaded structure (at desired temperature).
4. Computation of the necessary, time-averaged quantities (i.e., stresses, deformations, etc.).

The three last steps are repeated in the loop until desired final deformation is achieved. The additional equilibration of the deformed structure at each iteration of the algorithm drastically increases the time of the computations.

In this paper, the non-equilibrium molecular dynamics algorithm called SLLOD [33] is proposed to overcome this problem. Such an approach allows to simulate the atomic system under continuous strain, thus eliminating the necessity of time-consuming equilibration. Additionally, in this method considered molecular system can be easily coupled to the Nose-Hoover thermostat [15, 22]. In this case, the motion of the particles is determined by the following set of Hamilton's equations:

$$\begin{aligned}
\dot{\mathbf{q}}_i &= \frac{\mathbf{p}_i}{m_i} + \mathbf{q}_i \cdot \nabla \mathbf{u}, \\
\dot{\mathbf{p}}_i &= \mathbf{f}_i - \mathbf{p}_i \cdot \nabla \mathbf{u} - \frac{p_\eta}{Q}\mathbf{p}_i, \\
\dot{\eta} &= \frac{p_\eta}{Q}, \\
\dot{p}_\eta &= \sum_{i=1}^{N} \frac{p_i^2}{m_i} - dNk_BT.
\end{aligned} \tag{1}$$

The vectors $\mathbf{q}$ and $\mathbf{p}$ are the sets of the atomic coordinates and momenta, respectively. The $\mathbf{f}_i$ denotes force, acting on the i-th particle with mass m_i, while $\nabla \mathbf{u}$ refers to the strain rate of the system under continuous deformation. The d and N refer to the dimension of the problem and number of degrees of freedom, respectively. Symbol η is a time-dependant thermodynamic friction coefficient, T is the desired temperature of the system and the Q is the thermostat mass parameter defined as

$$Q = dNk_BT\tau^2, \tag{2}$$

where τ denotes relaxation time and k_B is the Boltzman constant.

Interactions between carbon atoms are computed using adaptive intermolecular reactive bond order (AIREBO) potential for hydrocarbons [31], a variant of the reactive empirical bond-order (REBO) model [3] with additional torsion and long range terms. Other possible approaches of modeling carbon-carbon interactions in the MD analysis utilize the ReaxFF force fields, based on the first-principles calculations [6] or the family of the so-called long-range carbon bond order potentials (LCBOP, LCBOPII) [18]. The AIREBO potential, used in this work, is fitted to handle different spatial configurations and hybridizations types of carbon atoms and is computationally more effective than the ReaxFF approach, which additionally requires shorter time step and equilibration of the atomic charge every certain number of iterations [20, 26]. However, the AIREBO potential treats the long range interactions in the simplified way because it utilizes simple Lennard-Jones-like function for computation of interactions of this type.

Series of tensile and shear tests for each presented allotrope are carried out at the temperature of 10 K with time step equal to 1 fs. Such a low temperature is chosen to limit vibrations of particles and fluctuations of the temperature itself. All the simulations are performed using three square graphene sheets of different sizes (approximately: 5×5, 10×10, 20×20 nm) for each allotrope due to examination of the size-dependence of the atomic domain. The real dimensions, numbers of atoms and densities of the 10×10 sheets are presented in Table 1. For the models of other sizes, these values are proportionally scaled. Periodic boundary conditions are imposed to avoid problems with unstable, unbalanced edges of the graphene sheet.

Table 1. Dimensions and densities of the investigated atomic models. The relative change of density was computed with respect to graphene sheet.

Structure 10×10	Dimensions [nm]	No. of atoms	Avg. density [atoms/nm^2]	Relative change of density
A	10.06×9.92	3936	39.4	0
B	11×10.8	3456	29	26%
C	10.5×9.93	2376	22.8	42%
D	9.97×9.87	1792	18.2	54%
E	10.3×10.7	3240	29.4	25%
F	10.3×10.4	2508	23.4	41%
G	10.2×10.2	3364	32	19%
H	10.3×10.3	3920	37	6%

In the first step, the energy minimization routine based on the Polak-Ribiere conjugated gradient algorithm is applied for each type and size of structure. Such an approach ensures that whole atomic structure will be sufficiently equilibrated (at zero temperature) and prepared for the further investigations. In the subsequent step the structure is heated from 0 K to 10 K with a constant rate of 0.1 K/ps to keep the fluctuations of the temperature as low as possible.

The tensile test is performed in the two perpendicular directions (see Fig. 1). In each run atomic lattice is stretched from 0% to 35% with continuous deformation with a strain rate corresponding to the velocity 10 m/s. In the case of shearing, the strain is applied from 0 degrees to 20 degrees with rate equal to 0.1 degree/ps.

The atomistic stress tensor is calculated using the adaptation of the classical virial theorem for the gas pressure [32]:

$$\boldsymbol{\sigma} = \frac{1}{\Omega}\sum_{i}^{N}\left[-m_i\mathbf{v}_i\otimes\mathbf{v}_i + \frac{1}{2}\sum_{j\neq i}^{N}\mathbf{r}_{ij}\otimes\mathbf{f}_{ij}\right], \tag{3}$$

where i and j are indices of the atoms, $\mathbf{v}_i$ is the velocity of the i-th particle and $\mathbf{f}_{ij}$ is the force acting between two particles. Summation is performed on all atoms occupying volume Ω, in this work –

on all atoms of the investigated structure. The virial stress theorem (3) has two parts: kinetic one and potential one and generally is not an equivalent of the Cauchy stress or any other macroscopic mechanical stress tensor. However, when the kinetic part of the virial equation is neglected and the values obtained in each integration step are averaged over the time and geometry, the atomistic stress may be reduced to the Cauchy stress with physical meaning [30, 35]. Additionally, in the present work, this way of computation of the stress tensor seems to be right, because the amount of kinetic energy is small, due to low temperature of the simulation. All quantities, necessary to obtain stress tensor, are averaged at every 500 time step.

The *ab-initio* calculations reveal isotropic properties of the graphene [17]. Additionally, under small deformations such a behavior can be successfully described by the continuum theory of linear elasticity. For the plane stress case, the stress-strain relation

$$\boldsymbol{\sigma} = D\boldsymbol{\varepsilon} \tag{4}$$

has the following form:

$$\begin{bmatrix} \sigma_x \\ \sigma_y \\ \tau_{xy} \end{bmatrix} = \frac{E}{1-\nu^2} \begin{bmatrix} 1 & \nu & 0 \\ \nu & 1 & 0 \\ 0 & 0 & \lambda \end{bmatrix} \begin{bmatrix} \varepsilon_x \\ \varepsilon_y \\ \gamma_{xy} \end{bmatrix}, \tag{5}$$

where $\lambda = (1-\nu)/2$. For uniaxial strain, e.g., along x axis, $\sigma_x \gg \sigma_y$ occurs, thus Eq. (5) can be simplified

$$\sigma_x = E\varepsilon_x \tag{6}$$

and in the similar way

$$\sigma_y = E\varepsilon_y, \tag{7}$$

$$\tau_{xy} = G\gamma_{xy}. \tag{8}$$

For the isotropic materials, the Young's modulus E, the shear modulus G and the Poisson's ratio ν are tied together by the following relation

$$\nu = \frac{E}{2G} - 1. \tag{9}$$

Elastic constants in the small deformation range can be easily determined computing the slope coefficient of the linear approximation of the stress-strain curve. In this paper all values of the elastic moduli are provided in the force per unit length (N/m) units, rather than commonly used force per unit area units (GPa). It is due to problems with evaluation of effective thickness and the energy of cohesion of the single sheet of each allotrope of graphene. For the basic, hexagonal network of graphene, (structure A) the cohesion energy is of order 260–498 mJ/m^2 and the effective thickness is known and equal to 3.34–3.35 Å [8, 11, 14, 17]. For the structure B values provided by different researches vary from 3.2 Å [7] to 3.51 Å [21] and additionally depend on the mutual spatial orientation of the sheets. For many other allotropes of graphene these values still remain unknown as well as spatial arrangements of the sheets, since differences between binding energies are too small to predict preferred orientation only by the basics of the computer simulations [21].

4. Results and analysis

In the first step, the equilibrium bond lengths of all types of the described structures are determined. The initial values are taken from [10]. Each created atomistic model was subjected to the energy minimization procedure, based on the conjugated gradient algorithm. After that, each structure is

checked that is fully relaxed, i.e., computed internal stress has a near-zero value. Obtained averaged equilibrium bond lengths for various types of hybridization of the carbon atoms are gathered in Table 2.

Table 2. Averaged equilibrium bond lengths (in Å) for the AIREBO potential (* additional test with the LCBOP potential).

Structure	sp^1–sp^1	sp^1–sp^2	sp^2–sp^2	sp^2–sp^3
A	–	–	1.41/1.42*	–
B	1.33	1.38	1.4	–
C	1.33	1.39	1.4	–
D	1.33	–	1.39	–
E	see	Text	and	Fig. 2
F	–	–	1.47	–
G	see	Text	and	Fig. 2
H	1.33	1.39	1.4	–
I	–	–	1.5	1.55

Determined values (for the 10×10 nm sheets with imposed periodic boundary conditions) are typical and are in the agreement with the results presented in the literature. It can be noted that the equilibrium bond length in the benzene ring depends on the model type, method of the simulation and applied force-field. For the braced-truss models with the AMBER and Morse potentials, the interatomic distance is equal to 1.38 Å [28], while the MD simulations with the ReaxFF predict the bond length in the aromatic benzene rings of the order of 1.49 Å [7]. Distances determined using the more accurate methods, based on the quantum mechanics, provide the values from 1.415 Å [17] to 1.427 Å [10]. Additionally, according to [9], the equilibrium lengths in the graphene sheets depend on the Stone-Wales defects and may vary between 1.37–1.54 Å.

Analogical situation occurs with the lengths of the bonds of the acetylenic linkages of the *graphyne*-like structures. The lengths of the single and the triple bonds vary between 1.38–1.48 Å and 1.19–1.35 Å, respectively, and depend on the atomistic model and method of the analysis [7, 10, 23]. One word should be said about equilibration (i.e., minimization of the potential energy) of the structures which contain square-shape elements: the types (G) and (E) (Fig 1). The bond analysis with the DFT-based tight-binding method [10] predicts the one, constant bond length: 1.429 Å and 1.449 Å for the structure (G) and (E), respectively. However, obtained results presented herein are slightly different (Fig. 2).

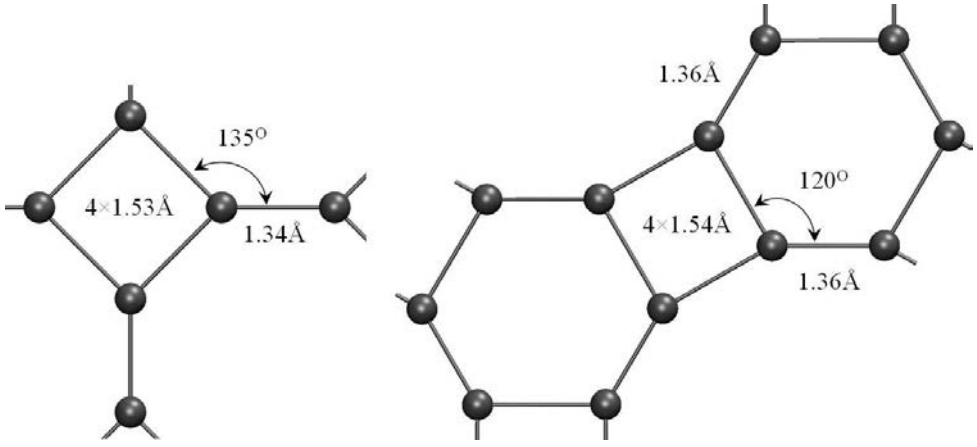

Fig. 2. The equilibrium bond lengths of structures (G) and (E).

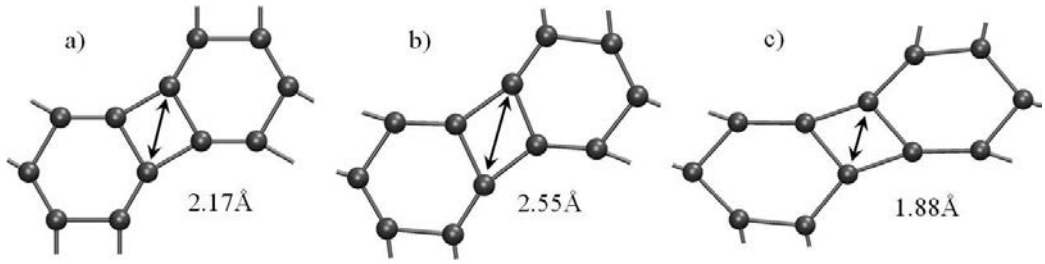

Fig. 3. Deformations of the structure (E) during tensile test. Diagonals were measured under approx.: a) 1%, b) 4% and c) 9% of strain.

The energy minimization of the lattices (G) and (E) with AIREBO interaction model results with constant lengths of the single bonds (C-C) of the square elements (approx: 1.535 Å) and shorter double bonds (C=C, respectively: 1.34 and 1.36 Å). This is due to various values of the angles between the sp^2 hybridized atoms (different than $3\times120^\circ$ in the graphene sheets). All characteristic angles of these structures, i.e., 135° in the octagons and 150° in the dodecagons, remain preserved. The allotrope (I) contains sp^2 and sp^3 hybridized atoms and obtained bond lengths between sp^2–sp^2 and sp^2–sp^3 atoms are larger than the other ones. Such results also correspond to the larger values presented in [10] (1.458 Å and 1.53 Å respectively). There are no problems with the structural stability of any examined graphene allotropes.

In the case of the MD simulations, the equilibrium distances also depend on the boundary conditions. Therefore, additional tests with equilibration of the 10×10 nm sheet of graphene with free edges, AIREBO and LCBOP potentials are performed. These simulations result in slightly larger interatomic distances equal to 1.413 Å and 1.425 Å, respectively for each type of the potential. This can partially (due to different reactive force field model) explain the larger bond lengths of the *graphyne* presented in [7], where non-periodic sheets were examined.

Series of tensile and shear tests are performed using three square sheets of different sizes for each allotrope. The stress-strain characteristics, presented in Figs. 4–12, are obtained for the molecular sheets of size 10×10 nm. All of the curves are plotted to the point of rupture of the first bonding. It can be noted that this phenomenon generally does not correspond to damage of the whole structure. Computed mechanical properties for the small strain range (0–3%) are summarized in Tables 3 and 4. The Poisson's ratio ν is computed using the relation (9) when the degree of anisotropy E_x/E_y was close to 1, i.e., considered structure reveals isotropic behavior in the two perpendicular directions.

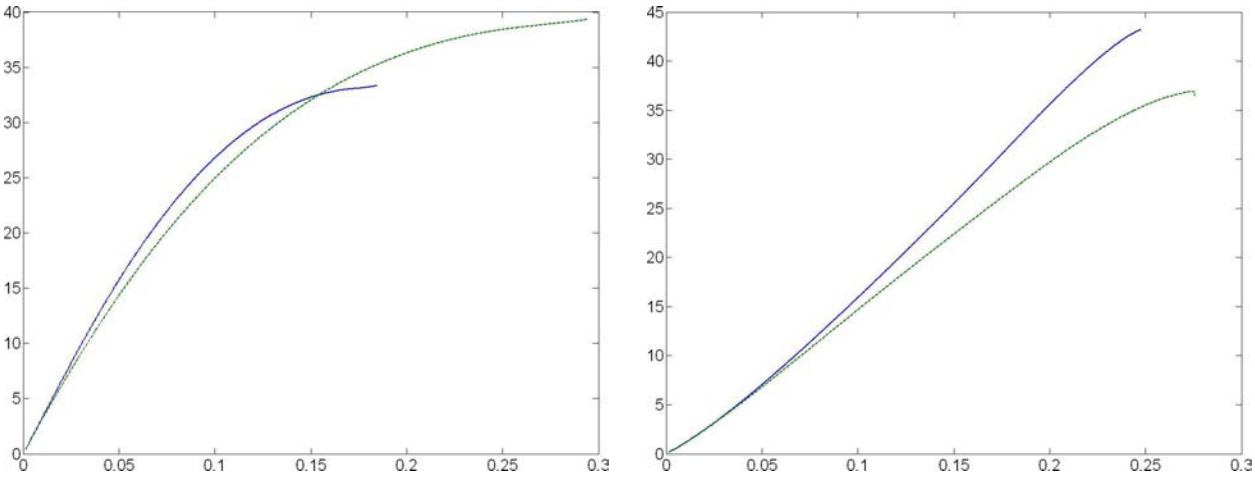

Fig. 4. Strain-stress curves of the graphene (A): tensile (left), shear (right). Solid and dashed lines denote zigzag and armchair directions, respectively.

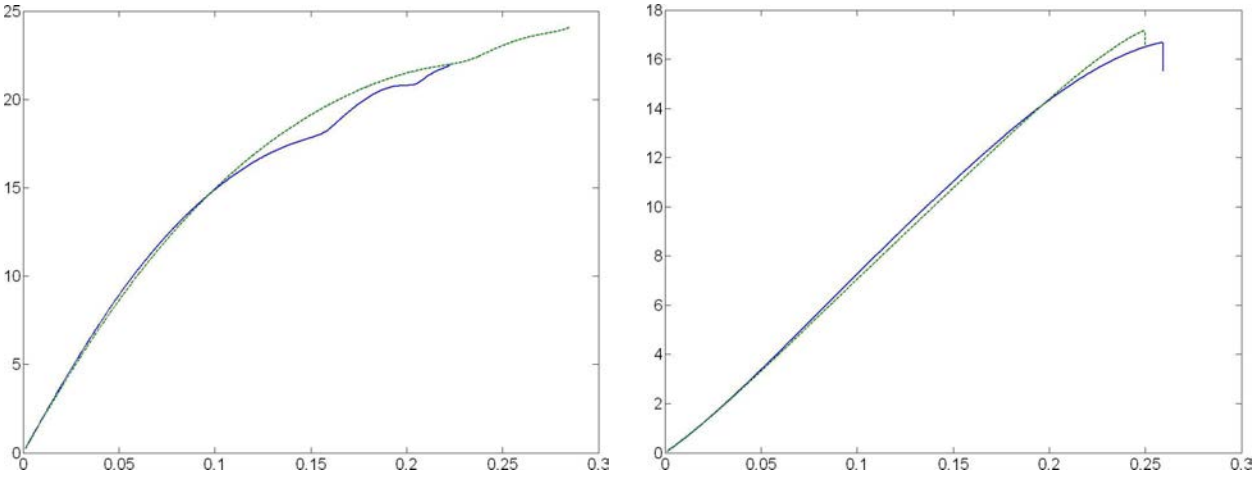

Fig. 5. Strain-stress curves of the graphyne (B): tensile (left), shear (right).
Solid and dashed lines denote zigzag and armchair directions, respectively.

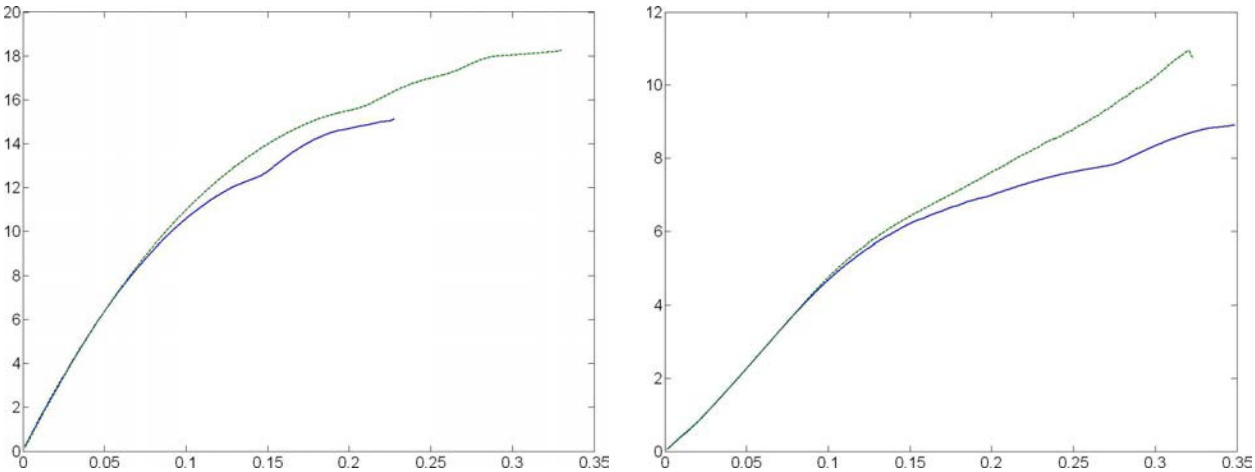

Fig. 6. Strain-stress curves of the graphidyne (C): tensile (left), shear (right).
Solid and dashed lines denote zigzag and armchair directions, respectively.

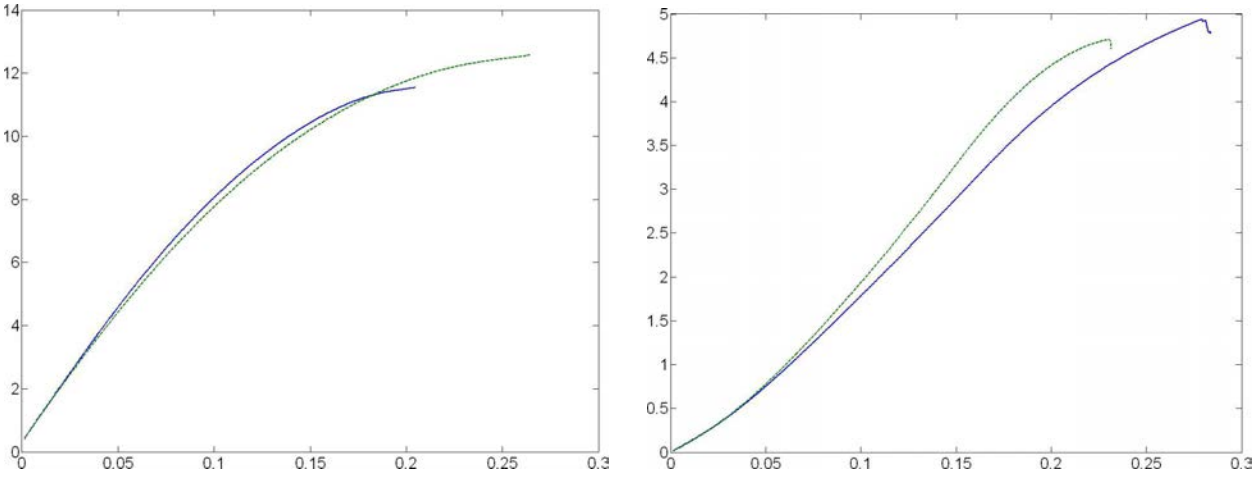

Fig. 7. Strain-stress curves of the structure D: tensile (left), shear (right).
Solid and dashed lines denote zigzag and armchair directions, respectively.

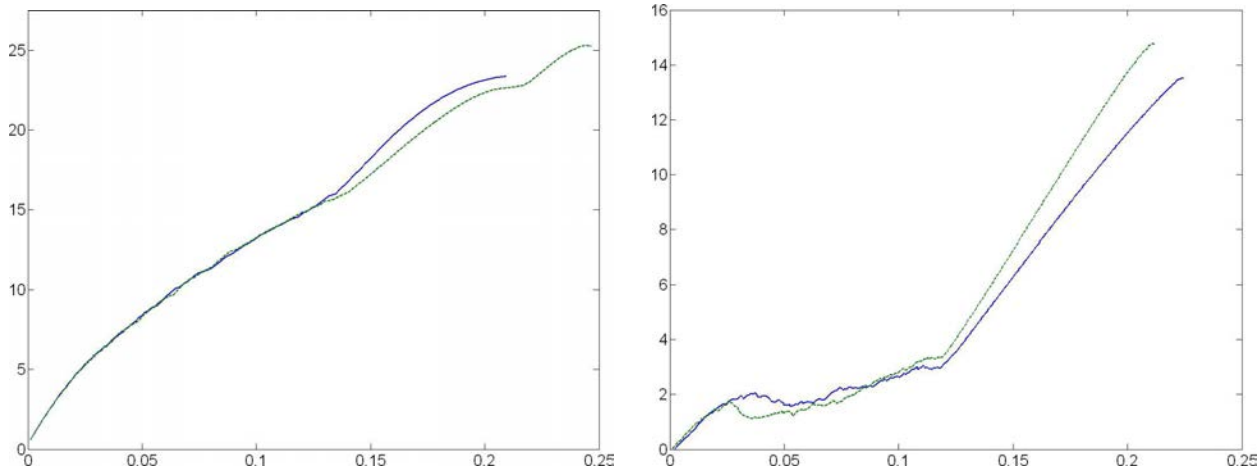

Fig. 8. Strain-stress curves of the structure E: tensile (left), shear (right). Solid and dashed lines denote strain along x and y axis, respectively.

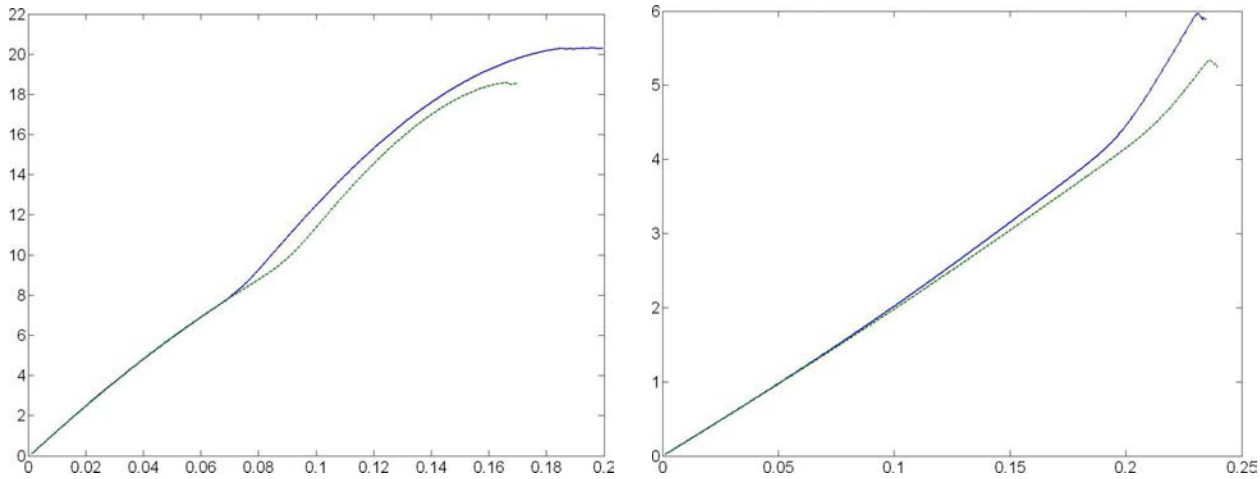

Fig. 9. Strain-stress curves of the structure F: tensile (left), shear (right). Solid and dashed lines denote strain along x and y axis, respectively.

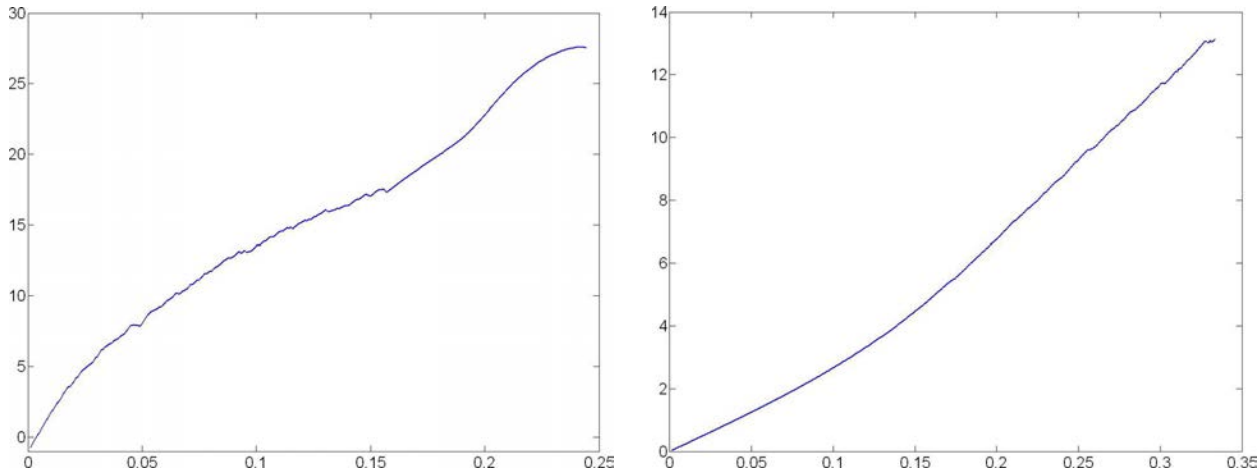

Fig. 10. Strain-stress curves of the structure G: tensile (left), shear (right).

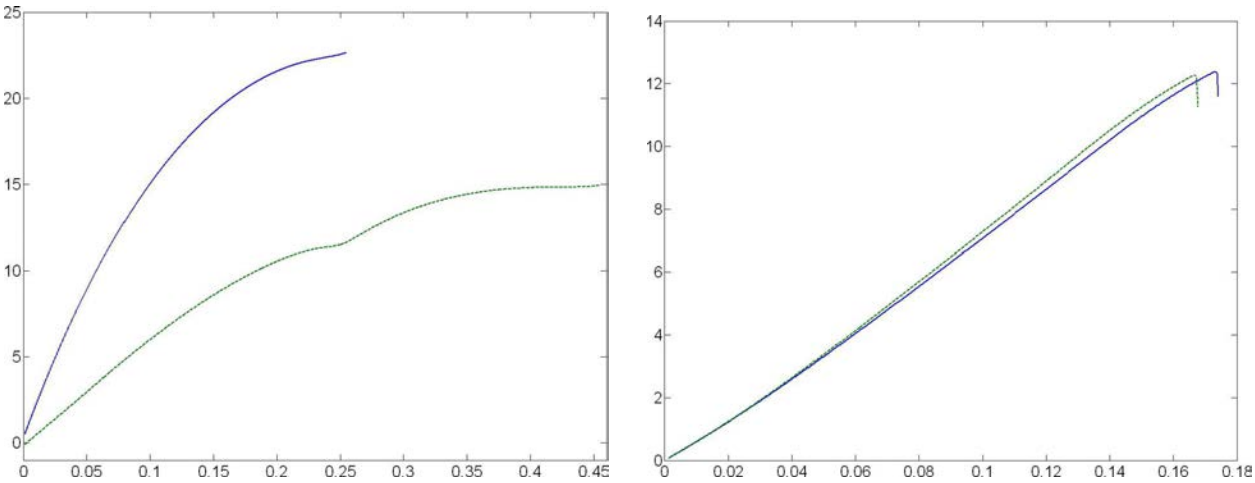

Fig. 11. Strain-stress curves of the structure H: tensile (left), shear (right). Solid and dashed lines denote strain along x and y axis, respectively.

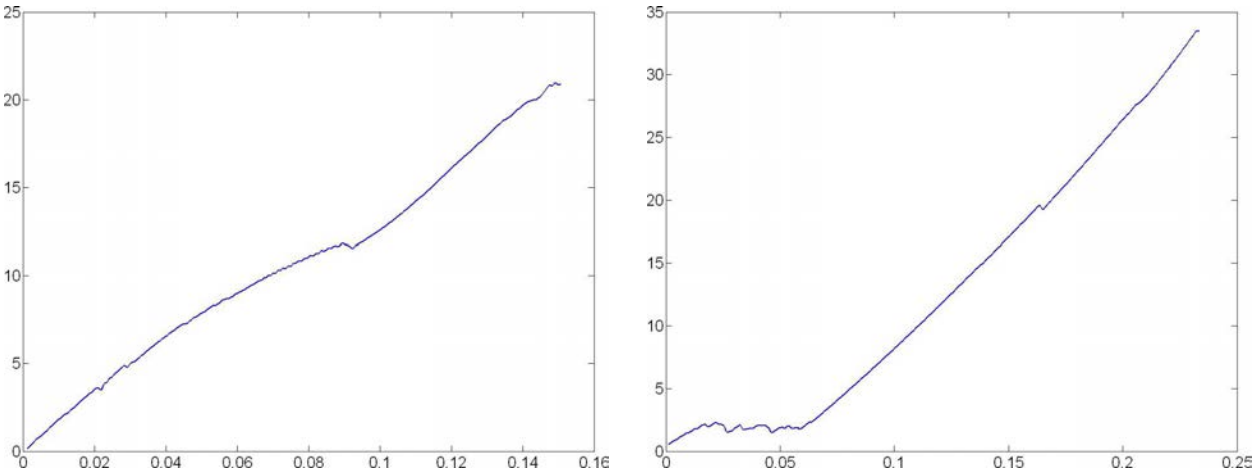

Fig. 12. Strain-stress curves of the structure I: tensile (left), shear (right).

Table 3. Mechanical properties of the 5×5 nm sheets (** results obtained with the REBO potential).

Structure	E_x [N/m]	G_{xy} [N/m]	ν_{xy}	E_y [N/m]	G_{yx} [N/m]	ν_{yx} [N/m]	E_x/E_y
A	330	131	0.26	306.5	128.7	0.19	1.08
B	182.4	47.5	0.9	181.8	46.8	0.94	1.003
C	135.5	41.8	0.62	134.8	43.3	0.6	1.005
D	85.35	12.7		88	12.8		0.97
E	214	68.9		148.6	60.4		1.44
F	124.8	19.4		124.5	19.4		1.002
G	260	21					
H	182.7	62.8		62	63.9		2.95
I	178.5 201**	114.6 110.2**	−0.22 −0.08**				

Table 4. Mechanical properties of the 10×10 nm sheets
(* results obtained for the LBOP potential, ** results obtained with the REBO potential).

Structure	E_x [N/m]	G_{xy} [N/m]	ν_{xy}	E_y [N/m]	G_{yx} [N/m]	ν_{yx} [N/m]	E_x/E_y
A	330 298*	131 127.5*	0.26 0.16*	307.2 294*	129 127.5*	0.19 0.15	1.07 1.01*
B	188.4	64.3	0.465	181	63.7	0.42	1.002
C	133.5	41.8	0.59	134.7	42	0.6	0.99
D	85	13.2		87.3	13.1		0.97
E	207.9	83.7	0.24	205	77.8	0.31	1.014
F	125	19.4		124.5	19.4		1.004
G	251	25.2					
H	182.6 172*	62.8 23*		62 54*	63.75 23.3*		2.945 3.18*
I	176.8 194**	111 87**	−0.2 0.13**				

The first investigated structure is the basic variant of the graphene (A), mainly due to large amount of data available in the literature, necessary to validate our models and the whole test suite. For the middle-sized sheet (10×10 nm) the obtained value of the Young's modulus equals 307.2 N/m in the armchair (y) direction and 330 N/m in the zigzag (x) direction. Assumption of the effective thickness of the sheet of 3.35 Å yields to the values of 917 GPa and 985 GPa, respectively. This gives an anisotropy coefficient $E_x/\underline{E}_y$ of 1.07. Generally, the graphene's elastic modulus is reported to be of order of 1 TPa, so these results are compatible with the ones presented in other works, however, in almost all cases graphene reveals an isotropic behavior in the small strain ranges. The results of the previous ReaxFF MD simulations [8] provide values of the 968 GPa and 957 GPa respectively in the armchair and zigzag directions while the DFT computations [17] yield the value of 1050 GPa in both directions. Similar values were summarized in the work [27]. On the opposite side, analysis of the braced-truss model with the Morse force field [28] results in even greater degree of anisotropy (0.71). In order to explain such an anisotropic behavior, the tensile and shear tests are repeated with the slower velocity (equal to 1 m/s), increased temperature (up to 100 K) and with the LCBOP potential, instead of previously used AIREBO. The changes of the elongation speed and temperature did not bring any new results. Such a behavior is in agreement with the MD simulations presented in [7], where the tensile tests with the strain rates in range of 0.5–10 m/s produce similar results. However, the same molecular model with LCBOP-based interactions reveals almost ideal isotropic properties (see Table 4), thus described phenomenon seems to be caused by unique features of the AIREBO potential.

The values of the ultimate stresses and strains as well as differences between stress-strain relations in the armchair and zigzag directions (Fig. 4) correspond to the ones presented in [8, 17]. Obtained value of the shear modulus is of order 130 N/m (388 GPa), with practically negligible difference between directions of deformation. In the open access literature, the value of the shear modulus depends on method, atomistic model, boundary conditions and varies widely in the range from 0.2 TPa to 1.76 TPa [8, 27, 28]. Due to introduced slight anisotropy, computed Poisson's ratios depend on the direction of the imposed strain. The averaged value is equal to 0.225 while the DFT computations predict the value of 0.186 [17]. Similarly to the shear modulus, the Poisson's ratios also depend on the adopted methodology of the investigations. A great juxtaposition is included in the paper [28].

The investigation of the properties of the *graphyne* sheet (B) predicts almost isotropic behavior in small strain range. The values of the Young's modulus and Poisson's ratio are of order 185 N/m and 0.44 for the 10 × 10 nm sheet, respectively. These results are slightly higher than the ones obtained

during DFT calculations ($E = 162.1$ N/m, $\nu = 0.417$) in the work [23]. However, computed ultimate strains also exceed 22%, while the other MD simulations with ReaxFF predict ultimate strains of order 8% and 13% along the armchair and zigzag directions [7]. Additionally, the molecular model based on ReaxFF potential reveals anisotrophy of the *graphyne*: an over-stiffness in the zigzag direction (elastic modulus of 224 N/m) while the stiffness along armchair directions has the similar value ($E = 170$ N/m). The obtained, averaged values of the shear modulus are of order 64 N/m. The values of the elastic and shear moduli are approximately 50% smaller than values obtained for the graphene while the Poisson's ratio is two times greater. It means that *graphyne* is a soft material, mainly due to lower atomic density of the structure compared to the graphene (Table 1).

Analogical situation occurs in the case of *graphidyne* (C), a derivative of the *graphyne* with the elongated acetylenic linkages (Fig. 1). The tensile and shearing tests reveal isotropic behavior, elastic and shear moduli of 134 N/m and 42 N/m, respectively and the Poisson's ratio approx. of 0.6. The ultimate strain in the armchair direction is larger than graphyne, due to orientation of the acetylenic chains, which are situated parallel to the armchair axis. It is hard to validate the results due to lack of available data (only the structural properties were available at that moment [10, 13]). Obtained values seem to be proper and acceptable when the sparse, spatial arrangement and low density of the *graphidyne* is taken into consideration. Similarly, the allotrope of type (D) – a honeycomb extended with acetylenic linkages, reveals the following properties: $E = 85$ N/m and $G = 13$ N/m, making this structure the softest of all presented in this paper. This lattice has also the lowest values of the ultimate stresses (Fig. 7) and the lowest number of atoms per unit area (Table 1).

The structure (E) has strong nonlinear tensile and shear characteristics presented in Fig. 8. When considering the range of the smallest strains (0–2%), computed Young's modulus is of the order of 205 N/m. Upon increasing strain, the stiffness decreases, so in the range of 2–6% is equal to approx. 120 N/m and further decreases to 88 N/m in the range of 6–12%. The shearing test reveals the "dead" region in the stress-strain characteristics. These phenomena, as well as changes in the stiffness, are caused by the slips and rearrangements of atoms during continuous deformation, which prevent deformation of angles between particles, especially in the square-shape interconnections between two hexagons in the unit cell (see Fig. 3 for details).

The tests performed on allotrope (F) results with the value of elastic modulus of 125 N/m and the shear modulus equal to 19.4 N/m. Such a low value and large disproportion between computed stiffness are due to specific mechanism of deformation in this structure: only the double bonds (i.e., connections between two triads of atoms in the unit cell, Fig. 1F) undergo the torsion, while the single-bonded triads of atoms remain virtually undeformed. The similar mechanism is responsible for even greater disproportion between tensile (251 N/m) and shearing (25 N/m) stiffness in the case of the lattice (G). In the small strain range, the double bonds bend under shearing, while the square elements still remain undeformed, while under the large axial strains ($< 15\%$), the square elements also start to elongate, thus the single bonds try to take the orientation parallel to the direction of the strain, which leads to subsequent increase of stiffness (Fig. 10). Such a behavior results with nonlinear tensile characteristics, similar to the ones obtained for structure (F).

The only allotrope of graphene which revealed strong anisotropic behavior is the type (H). This structure is similar to the type (D) but the vertical acetylenic linkages are replaced with the double bonds between the sp^2 hybridized carbon atoms. The anisotrophy is caused by the orientation of the each type of bonds in respect to the directions of the applied strain. The acetylenic chains create acute angles of 30° and 60° with the x and y axis, respectively, while the double bonds are directly subjected to the tensile strain only in the armchair (y) direction (according to Fig. 1). Similarly like in the lattice (G), upon applied strain in the zigzag direction (i.e., x axis), the acetylenic linkages slowly stretch and turn the alignment to the direction of the strain. The double bonds prevent this process. This results with a high stiffness of the order of 182 N/m. In the armchair direction, the deformation of the acetylenic linkages runs easier, due to wide angle between each pair of them, additionally the double bonds stretch themselves. Thus, the resultant stiffness in the armchair direction is approximately three times lower (62 N/m). The shear modulus has constant

value of 63 N/m in both directions. The tensile tests were repeated with the LCBOP potential and yield similar Young's modulus (Table 4), but the values obtained during shearing were three times smaller. It is due to different ways of handling of the angular interactions (i.e., torsion of bondings) by these potentials. It can be noted that in the case of such a behavior the equations of isotropic elasticity (1.4–1.9) are no longer valid and have to be replaced with the ones for 2D orthotropic material.

The last structure taken into investigation, type (I), contains the four-fold, in-plane sp^3 hybridized atoms, thus proved to be more challenging configuration for the parameterized empirical potentials. The test suite was performed using the LCBOP (first version), REBO and AIREBO potentials. In the first case, the structure becomes unstable shortly after beginning of the simulation. The LCBOP potential does not handle such a planar network properly, since it was fitted only for the carbon chains and 3D structures such as diamond and graphite. The last two models of carbon interactions contain many-body terms fitted to describe symmetric, quadruple coordinated atoms properly. The results are presented in Tables 3–5, and the stress-strain curves are shown in Fig. 12. The stiffness, obtained during tensile test of the 10×10 nm sheet, is similar (177 N/m for AIREBO vs. 186 N/m in the case of REBO potential); however, the bigger difference was shown in the test of shearing. The following values of the shear modulus were determined: 111 N/m and 87 N/m for the AIREBO and REBO models, respectively. This difference is mainly caused by the lack of the torsion term in the REBO potential formulation.

Table 5. Mechanical properties of the 20×20 nm sheets
(** results obtained with the REBO potential).

Structure	E_x [N/m]	G_{xy} [N/m]	ν_{xy}	E_y [N/m]	G_{yx} [N/m]	ν_{yx} [N/m]	E_x/E_y
A	330.8	130.6	0.267	308	129	0.19	1.07
B	188.5	64.2	0.47	181	63.7	0.42	1.04
C	136.2	45.1	0.51	134.5	45.1	0.49	1.01
D	84.5	13.25		87.4	13.4		0.97
E	196	69.3	0.41	202.9	71.2	0.42	0.97
F	124.9	19.4		124.5	19.4		1.003
G	262.1	25.1					
H	182.4	62.9		61.9	63.8		2.95
I	185.1 210**	121 93**	−0.26 0.13				

The results, generally, do not depend on the size of the atomistic model. In a several cases (like in the smallest *graphyne* and (I)-type sheets), some differences occur, probably due to influence of pseudo-randomly generated set of the atom's velocities and artificial periodicity [16], introduced to the small and sparse molecular model surrounded by the periodic boundaries.

The surges, visible on some strain-stress graphs (e.g., ones of the *graphyne* and *graphidyne* under large strains) are due to switching of the distance-dependant terms in the atomic potential and simplified long range interaction model (treated as a simple Lennard-Jones function). The switching mechanism is a characteristic feature of the applied bond-order potentials.

5. General conclusions

The series of tensile and shear tests of the nine types of the flat carbon networks were performed. The strain-stress characteristics and equivalent mechanical parameters were determined. In the case of *graphyne* and *graphidyne* structures, results of the investigations are in good agreement with information available in the open access literature. Note, in most cases this was a comparison

of the results yielded by fast MD with the empirical atomic potential with more accurate, but computationally extensive, quantum calculations. Other results presented in this paper were analyzed and discussed in detail. The AIREBO potential seems to be reasonable choice for modeling of the presented flat carbon structures, where the *ab-initio* methods are not an option, such as large models up to hundreds of thousands of atoms or complex systems made of carbon networks. The described test suite will be extended with the ReaxFF or LCBOPII potential, which should solve the long range interaction problem and make additional validation of the presented results possible.

Except the structure (H), all of examined lattices reveal isotropic behavior under small strains, however it is possible to build new carbon networks with unique properties from the basic elements (benzene rings, triads, acetylenic groups, etc.) and determine their properties using the presented methodology. The obtained mechanical properties complement the structural and electronic data, which have been already presented in the works like [2, 10, 13, 36] and can be used, e.g., in the multi- and meso-scale modeling, numerical homogenization and nano-engineering.

Acknowledgment

Financial support of the NCBiR, project no. R07 0006 10, is acknowledged.

References

[1] M. Arroyo, T. Belytschko. Finite crystal elasticity of carbon nanotubes based on the exponential Cauchy-Born rule. *Physical Review B*, **69**(11): 115415, 2004.

[2] R.H. Baughman, H. Eckhardt, M. Kertesz. Structure-property predictions for new planar forms of carbon: Layered phases containing sp^2 and *sp* atoms. *The Journal of Chemical Physics*, **87**(11): 6687–6699, 1987.

[3] D.W. Brenner, O.A. Shenderova, J.A. Harrison, S.J. Stuart, B. Ni, S.B. Sinnott.A second-generation reactive empirical bond order (REBO) potential energy expression for hydrocarbons. *Journal of Physics: Condensed Matter*, **14**: 783–802, 2002.

[4] M.J. Bucknum, E.A. Castro. The squarographites: A lesson in the chemical topology of tessellations in 2- and 3-dimensions. *Solid State Sciences*, **10**: 1245–1251, 2007.

[5] T. Burczyński, A. Mrozek, R. Górski, W. Kuś. The molecular statics coupled with the subregion boundary element method in multiscale analysis. *International Journal for Multiscale Computational Engineering*, **8**(3): 319–330, 2010.

[6] K. Chenoweth, A.C.T. van Duin, W.A. Goddard. ReaxFF Reactive force field for molecular dynamics simulations of hydrocarbon oxidation. *Journal of Physical Chemistry*, **A**(112): 1040–1053, 2008.

[7] S.W. Cranford, M.J. Buehler. Mechanical properties of graphyne. *Carbon*, **49**: 4111–4121, 2011.

[8] S.W. Cranford, M.J. Buehler. Twisted and coiled ultralong multilayer graphene ribbons. *Modelling and Simulation in Materials Science and Engineering*, **19**: 2011.

[9] E. Duplock, M. Scheffler, P.J.D. Lindan. Hallmark of perfect graphene. *Physical Review Letters*, **92**: 225502, 2004.

[10] A.N. Enyashin, A.L. Ivanovskii. Graphene allotropes. *Physica Status Solidi*, **248**(8): 1879–1883, 2011.

[11] L.A. Girifalco, R.A. Lad. Energy of cohesion, compressibility, and the potential energy functions of the graphite system. *The Journal of Chemical Physics*, **25**(4): 693–697, 1956.

[12] M. Griebel, S. Knapek, G. Zumbusch. *Numerical simulation in molecular dynamics: numerics, algorithms, parallelization, applications*. Texts in Computational Science and Engineering, 5, Springer, 2007.

[13] M.M. Haley. Synthesis and properties of annulenic subunits of graphyne and graphdiyne nanoarchitectures. *Pure and Applied Chemistry*, **80**(3): 519–532, 2008.

[14] D.J. Henry, G. Yiapanis, E. Evans, I. Yarovsky. Adhesion between graphite and modified polyester surfaces: a theoretical study. *The Journal of Chemical Physics B*, **109**: 17224–17231, 2005.

[15] W.G. Hoover. Canonical dynamics: Equilibrium phase-space distributions. *Physical Review A*, **31**(3): 1695–1697, 1985.

[16] W.K Liu, S. Jun, D. Qian. Computational nanomechanics of materials, Handbook of theoretical and computational nanotechnology. M. Rieth and W. Schommers [Eds.], American Scientific Publishers, Stevenson Ranch, 2005.

[17] F. Liu, P. Ming, J. Li. *Ab initio* calculation of ideal strength and phonon instability of graphene under tension. *Physical Review B*, **86**: 064120, 2007.

[18] J.H. Los, L.M. Ghiringhelli, E.J. Meijer, A. Fasolino. Improved longrange reactive bond-order potential for carbon I. *Construction, Physical Review B*, **72**(21): 214102, 2005.

[19] K. Mylvaganam, L.C. Zhang. Nano-friction of some carbon allotropes. *Journal of Computational and Theoretical Nanoscience*, **7**(10): 1–4, 2010.
[20] A. Nakano. Parallel multilevel preconditioned conjugate-gradient approach to variable-charge molecular dynamics. *Computer Physics Communications*, **104**: 59–69, 1997.
[21] N. Narita, S. Nagai, S. Suzuki, K. Nakao. Electronic structure of three-dimensional graphyne. *Physical Review B*, **62**(16): 11146–11151, 2000.
[22] S. Nose. A unified formulation of the constant temperature molecular dynamics methods. *The Journal of Chemical Physics*, **81**(1): 511–519, 1984.
[23] Q. Peng, W. Ji, S. De. Mechanical properties of graphyne monolayers: a first-principles study. *Physical Chemistry Chemical Physics*, **14**(38): 13385–13391, 2012.
[24] Z. Qi, F. Zhao, X. Zhou, Z. Sun, H.S. Park, H. Wu. A molecular simulation analysis of producing monatomic carbon chains by stretching ultranarrow graphene nanoribbons. *Nanotechnology*, **21**: 265702, 2010.
[25] D. Rapaport. *The art of molecular dynamics simulation*. Cambridge University Press, UK, 2004.
[26] A.K. Rappe, W.A. Goddard III. Charge equilibration for molecular dynamics simulations. *The Journal of Chemical Physics*, **95**(8): 3358–3363, 1991.
[27] A. Sakhaee-Pour. Elastic properties of single-layered graphene sheet. *Solid State Communications*, **149**: 91–95, 2009.
[28] F. Scarpa, S. Adhikari, A.S. Phani. Effective elastic mechanical properties of single layer graphene sheets. *Nanotechnology*, **20**, 2009.
[29] O. Shenderova, D. Brenner, R.S. Ruoff. Would diamond nanorods be stronger than fullerene nanotubes? *Nano Letters*, **3**(6): 805–809, 2003.
[30] S. Shengping, S.N. Atluri. Atomic-level stress calculation and continuum-molecular system equivalence. *Computer Modeling in Engineering & Sciences*, **6**(1): 91–104, 2004.
[31] S.J. Stuart, A.B. Tutein, J.A. Harrison. A reactive potential for hydrocarbons with intermolecular interactions. *The Journal of Chemical Physics*, **112**(14): 6472–6486, 2000.
[32] D.H. Tsai. The virial theorem and stress calculation in molecular dynamics. *The Journal of Chemical Physics*, **70**(3): 1375–1382, 1979.
[33] M.E. Tuckerman, Ch.J. Mundy, S. Balasubramanian, M.L. Klein. Modified nonequilibrium molecular dynamics for fluid flows with energy conservation, *The Journal of Chemical Physics*, **106**(13): 5615–5621, 1997.
[34] Z. Zhao, B. Xu, X-F. Zhou, L.-M. Wang, B. Wen, J. He, Z. Liu, H.-T. Wang, Y. Tian. Novel superhard carbon: C-centered orthorhombic C_8. *Physical Review Letters*, **107**: 215502, 2011.
[35] M. Zhou. *A new look at the atomic level virial stress: on continuum-molecular system equivalence*. Proceedings of the Royal Society of London series A – Mathematical Physical and Engineering Sciences, **459**(2037): 2347–2392, 2003.
[36] H. Zhu, A.T. Balaban, D.J. Klein, T.P. Zivkovic. Conjugated-circuit computations on two-dimensional carbon networks. *The Journal of Chemical Physics*, **101**(6): 5281–5292, 1994.
[37] Q. Zhu, A.R. Oganov, M.A. Salvadó, P. Pertierra, A.O. Lyakhov. Denser than diamond: Ab initio search for superdense carbon allotropes. *Physical Review B*, **83**: 193410, 2011.